



**University of Dundee**

## **Microwave hydrothermal synthesis of tobermorite for the solidification of iron**

Luo, Shuqiong; Jiang, Zhuangzhuang; Zhao, Minghui; Yang, Lei; Castro-Gomes, João; Wei, Shihua

*DOI:*  
[10.1016/j.cscm.2023.e02267](https://doi.org/10.1016/j.cscm.2023.e02267)

*Publication date:*  
2023

*Licence:*  
CC BY-NC-ND

*Document Version*  
Publisher's PDF, also known as Version of record

[Link to publication in Discovery Research Portal](#)

*Citation for published version (APA):*  
Luo, S., Jiang, Z., Zhao, M., Yang, L., Castro-Gomes, J., Wei, S., & Mi, T. (2023). Microwave hydrothermal synthesis of tobermorite for the solidification of iron. *Case Studies in Construction Materials*, 19, Article e02267. <https://doi.org/10.1016/j.cscm.2023.e02267>

### **General rights**

Copyright and moral rights for the publications made accessible in Discovery Research Portal are retained by the authors and/or other copyright owners and it is a condition of accessing publications that users recognise and abide by the legal requirements associated with these rights.

### **Take down policy**

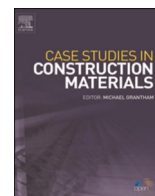
If you believe that this document breaches copyright please contact us providing details, and we will remove access to the work immediately and investigate your claim.



ELSEVIER

Contents lists available at ScienceDirect

## Case Studies in Construction Materials

journal homepage: [www.elsevier.com/locate/cscm](http://www.elsevier.com/locate/cscm)

Case study

## Microwave hydrothermal synthesis of tobermorite for the solidification of iron

Shuqiong Luo<sup>a</sup>, Zhuangzhuang Jiang<sup>a</sup>, Minghui Zhao<sup>a</sup>, Lei Yang<sup>a</sup>,  
João Castro-Gomes<sup>b</sup>, Shihua Wei<sup>c</sup>, Tangwei Mi<sup>c,\*</sup><sup>a</sup> Henan Key Laboratory of Materials on Deep-Earth Engineering, School of Materials Science and Engineering, Henan Polytechnic University, Jiaozuo 454003, PR China<sup>b</sup> Centre of Materials and Building Technologies (C-MADE/UBI), Department of Civil Engineering and Architecture, University of Beira Interior (UBI), 6201-001 Covilhã, Portugal<sup>c</sup> School of Civil and Environmental Engineering, Nanyang Technological University, 50 Nanyang Avenue, 639798, Singapore

## ARTICLE INFO

## Keywords:

Microwave hydrothermal synthesis  
Heavy metal  
Tobermorite  
Fe-tobermorite

## ABSTRACTS

Iron is one of the heavy metals that present in industrial wastewater and domestic waste which damage agricultural production as well as the landscape if there is no proper treatment. One popular method was to introduce the heavy metal ions into the raw material for the synthesis of tobermorite, as the main cement component. However, the conventional hydrothermal synthesis was time and intense energy consuming. Therefore, microwave hydrothermal synthesis of tobermorite was evaluated by comparing with the conventional method. The experimental results showed that the dominant products were Fe-tobermorite/ tobermorite via conventional method, whilst it turned to be Fe-containing hydrogarnet under microwave hydrothermal synthesis when the Fe/Si ratio was 0.15/0.2, which were found to be more stable, thus enhancing the safety of the solidification. Both methods exhibited 100 % of solidification of iron, and the microwave hydrothermal synthesis consumed a much shorter time than conventional method. Therefore, present work has demonstrated that microwave hydrothermal synthesis of tobermorite is an effective alternative to conventional method for the solidification of iron.

## 1. Introduction

Iron is an essential nutrient for humans and organisms, and its functions for the human body are manifested in many ways, such as its involvement in the transport and storage of oxygen, promoting development, increasing resistance to disease, and regulating tissue respiration [1]. Therefore, iron itself is not a significant contaminant. However, iron from industrial wastewater and domestic waste will occupy agricultural land and damage agricultural production as well as the landscape and vegetation without proper treatment [2]. Therefore, various techniques were developed to solidify the iron ions, especially for the treatment of industrial wastewater containing Fe<sup>3+</sup>. The current treatment methods include chemical precipitation method, biological method and membrane separation [3,4], which are, however, suffer from their high cost and low efficiency, as well as secondary pollution problems.

Solidification of heavy metal ions by tobermorite has been proved to be an effective method by introducing the heavy metal ions into the raw material for the synthesis of tobermorite [5]. Theoretically, the microstructure of tobermorite is modelled on the

\* Corresponding author.

E-mail address: [tangwei.mi@ntu.edu.sg](mailto:tangwei.mi@ntu.edu.sg) (T. Mi).<https://doi.org/10.1016/j.cscm.2023.e02267>

Received 13 May 2023; Received in revised form 23 June 2023; Accepted 1 July 2023

Available online 1 July 2023

2214-5095/© 2023 The Authors. Published by Elsevier Ltd. This is an open access article under the CC BY-NC-ND license (<http://creativecommons.org/licenses/by-nc-nd/4.0/>).

dreierketten model [6], where silica-oxygen tetrahedra on both sides are connected to Ca-O lamellae parallel to the b-axis and stacked along the c-axis to form a crystal of tobermorite, with the presence of water molecules and  $\text{Ca}^{2+}$  acting as equilibrium between the layers, i.e. forming an intermediate layer [5]. The Ca-O lamellae have a coordination number of 7 for Ca. The non-bridging silicon-oxygen tetrahedra (P) are paired silicon-oxygen tetrahedra to share 2 vertices, and the bridging silicon-oxygen tetrahedra (B) are silicon-oxygen tetrahedra connecting the non-bridging silicon-oxygen tetrahedra [5,7]. There are five  $\text{Ca}^{2+}$  in the molecular structure of tobermorite, where four  $\text{Ca}^{2+}$  form Ca polyhedra to produce the laminar structure of tobermorite, and the other  $\text{Ca}^{2+}$  and  $\text{H}_2\text{O}$  molecules form the intermediate layer in the crystal structure of tobermorite. When preparing tobermorite internal doping metal ions, such as  $\text{Fe}^{3+}$  and  $\text{Al}^{3+}$ , to produce metal-substituted tobermorite, the  $\text{Si}^{4+}$  ions are replaced to obtain a structure that is similar to tobermorite [8–10]. Such manner has been proved by previous work [11], where aluminium-substituted tobermorite was synthesized from waste blast furnace slag, sodium silicate and sodium hydroxide.

Currently, the conventional hydrothermal method is still a dominant synthesis method of tobermorite which is, however, both time and energy consuming [12,13]. To reduce the  $\text{CO}_2$  emissions during this process, microwave hydrothermal synthesis is a promising method that combines the conventional hydrothermal synthesis method with microwave fields, taking full advantage of both microwave and hydrothermal methods [14]. By comparing with conventional hydrothermal synthesis, microwave heating is featured with strong penetrating power, resulting in fast heating rate [15]. Therefore, microwave hydrothermal synthesis requires only few hours for synthesis of tobermorite, reducing the preparation time and energy consuming significantly [16]. In addition, the non-thermal effect of microwave heating can also reduce the activation energy of the reaction, making the preparation temperature lower than the that required by conventional heating methods [16]. Though synthesis of heavy metal substituted tobermorite via microwave hydrothermal seems superior to conventional method, the efficiency and feasibility of microwave hydrothermal synthesis of Fe-substituted tobermorite has been rarely reported in the literature as most work was related to Al-substituted tobermorite [17,18].

This work thus completed an attempt to employ advantageous microwave hydrothermal synthesis technology to produce Fe-substituted tobermorite by using calcium hydroxide, silicon dioxide and ferric trichloride hexahydrate as raw materials. The chemical and physical properties of the products via both microwave and conventional hydrothermal synthesis were thoroughly compared. The efficiency to solidify iron by these two methods were evaluated as well by determining the iron concentration in the supernatant and leaching solution. Finally, the effect of synthesis method and duration on the products was discussed in an attempt to provide some technical guidance and theoretical reference for the effective treatment of iron-containing waste.

## 2. Experiments

### 2.1. Materials

The chemicals used in this work include fumed silica ( $\text{SiO}_2$ ) from Degussa AG., and calcium hydroxide ( $\text{Ca}(\text{OH})_2$ , 95 %) and ferric chloride hexahydrate ( $\text{FeCl}_3 \cdot 6\text{H}_2\text{O}$ , 99 %) from Maclean. The deionised (DI) water was employed for dissolution and synthetization.

### 2.2. Sample preparation

$\text{Ca}(\text{OH})_2$ ,  $\text{SiO}_2$  and  $\text{FeCl}_3 \cdot 6\text{H}_2\text{O}$  were used as raw materials and mixed well at a Ca/(Si+Fe) of 0.83, Fe/Si of 0, 0.05, 0.1, 0.15 and 0.2, respectively, and a liquid to solid ratio of 30 mL/g. The mixed slurry was placed in a microwave digestion apparatus (Nanjing Xian'ou Instrument Manufacturing Co., Ltd, China) as shown in Fig. 1, and a dynamic hydrothermal reactor (GCF) produced by Dalian Automatic Control Equipment Factory as shown in Fig. 2 for synthesis tests. When the reaction was completed, the slurry was cooled to



Fig. 1. The diagram of dynamic hydrothermal reactor (GCF).

room temperature, and the supernatant was collected. In the meantime, the remaining sample was washed by filtration, and the resulting solid sample was dried under vacuum at 60 °C for 24 h. The experimental conditions for microwave and conventional hydrothermal synthesis are shown in Tables 1 and 2, respectively. The temperature and duration of synthesis was based on primary trial tests [19].

### 2.3. Microstructure

The mineral composition was characterised by a Smart-lab type XRD test with CuK $\alpha$  radiation (Rigaku Corporation of Japan). The scanning range was from 5° to 65° with a speed of 5°/min [20]. A Merlin Compact field emission scanning electron microscope produced by Carl Zeiss NTS GmbH, Germany was used to observe the microscopic morphology of the product. TG-DSC test was carried out on the sample using STA800 produced by Perkin Elmer Company. The experiment was carried out under nitrogen atmosphere, and the temperature was heated from 50 °C to 1000 °C with a heating rate of 5°/min. FTIR measurement was performed with a Bucks HP9 2FX thermal infrared spectrometer from Perkin Elmer, with a test range of 400–4000 cm<sup>-1</sup> and a resolution of 2 cm<sup>-1</sup>.

### 2.4. Heavy metal toxicity leaching experiment

To determine the heavy metal solidification effectiveness during synthesis, the concentration of iron ions in supernatant after hydrothermal synthesis were characterized by an iCAP Pro X inductively coupled plasma emission spectrometer (ICP-OES) from Thermo Fisher Scientific. In addition to the supernatant, the safety of the products synthesized by different methods, as the solidified body, were evaluated for heavy metal leaching toxicity according to a standard procedure named 'Solid Waste Leaching Toxicity Leaching Method - Horizontal Oscillation Method' as described in the literature [21,22]. The experiments were carried out under an argon atmosphere. The instrument was operated at 1150 W, with a cooling gas flow rate of 12.5 L/min, an auxiliary gas flow rate of 0.5 L/min and a pump speed of 45 rpm. The supernatant was filtered using a 0.45  $\mu$ m membrane.

## 3. Results and discussion

### 3.1. XRD: physical phase of the products

Fig. 3 shows the XRD patterns of samples prepared with different Fe/Si ratios at 2 h of microwave hydrothermal synthesis. It can be seen that the main phases of the sample were tobermorite when no iron was incorporated. When the Fe/Si ratio was 0.05, the main phase of the sample was Fe-tobermorite/tobermorite. Fe-containing hydrogarnet started to appear in the when the Fe/Si ratio reached 0.1. At an Fe/Si ratio of 0.15 and 0.2, reinhardbraunsite (Ca<sub>5</sub>(SiO<sub>4</sub>)<sub>2</sub>(OH)<sub>2</sub>) and gyrolite were detected in the hydration products of the sample. It is worth noting that, with the increase of Fe/Si ratio, the contents of Fe-containing hydrogarnet and gyrolite were found to increase, and, inversely, Fe-tobermorite/tobermorite was reduced based on the intensity of their corresponding diffraction peaks. Under hydrothermal reaction conditions, iron took the place of some of the silicon to form iron-substituted C-S-H, which formed as iron-substituted tobermorite and Fe-containing hydrogarnet [20]. Similar results were found in the literature [9].

Fig. 4 shows the XRD patterns of samples prepared with different Fe/Si ratios at 4 h of microwave hydrothermal synthesis. As can be seen from the figure, with the increase of Fe/Si ratio, the trend of the reaction products in the samples was generally similar to that in Fig. 3. The only difference was the appearance of gyrolite and Fe-containing hydrogarnet after 4 h of microwave hydrothermal synthesis at a Fe/Si ratio of 0.05. It is thus suspected that at longer curing times, the formation of the gyrolite and Fe-containing hydrogarnet was promoted even though there was a low Fe/Si ratio.

Fig. 5 shows the XRD patterns of the samples produced with different Fe/Si ratios after 14 h of conventional hydrothermal



Fig. 2. The diagram of microwave digestion apparatus (ATPIO-24 T).

**Table 1**  
Experiments under microwave hydrothermal conditions.

Sample No.	Ca/(Si+Fe)	Fe/Si	Liquid solid ratio (mL/g)	Synthesis temperature (°C)	Synthesis time (h)
M-T	0.83	0	30	220	2, 4
M-T-0.05Fe		0.05			
M-T-0.1Fe		0.10			
M-T-0.15Fe		0.15			
M-T-0.2Fe		0.20			

**Table 2**  
Experiments under conventional hydrothermal conditions.

Sample No.	Ca/(Si+Fe)	Fe/Si	Liquid solid ratio (mL/g)	Synthesis temperature (°C)	Synthesis time (h)
C-T	0.83	0	30	220	14
C-T-0.05Fe		0.05			
C-T-0.1Fe		0.10			
C-T-0.15Fe		0.15			
C-T-0.02Fe		0.20			

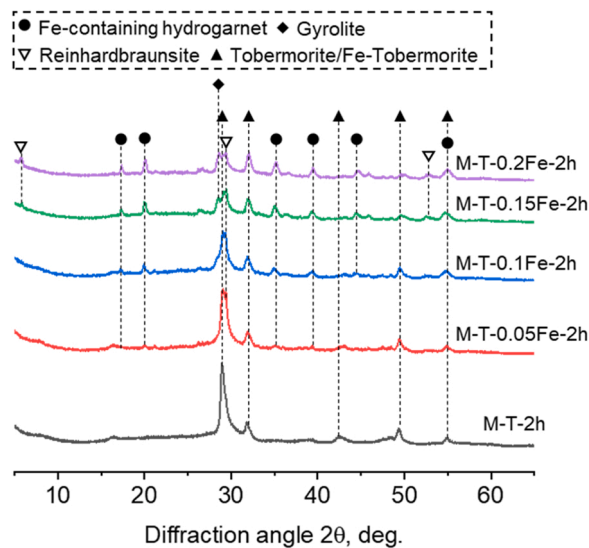


Fig. 3. XRD patterns of samples prepared with different ratios of Fe/Si after microwave hydrothermal synthesis for 2 h.

synthesis. With no addition of iron, the main physical phase of the sample was tobermorite, the diffraction peaks of tobermorite were more intensive than those for the samples after microwave hydrothermal synthesis. With an Fe/Si ratio of over 0.05, Fe-tobermorite and gyrolite and reinhardbraunsite appeared in the product. By comparing with the products after microwave hydrothermal synthesis, Fe-containing hydrogarnet was missing in the products after conventional hydrothermal synthesis.

### 3.2. SEM: morphologies of the products

Figs. 6 and 7 show the morphologies of samples produced by microwave hydrothermal synthesis for 2 h and 4 h, respectively. Generally, the morphologies of the products were generally similar to each other after 2 and 4 h with the sample Fe/Si ratio. As can be seen from Figs. 6(a) and 7(a), the samples were in the form of small flakes stacked together in a honeycomb pattern without iron, suggesting the presence of tobermorite [23]. The only difference was observed when the Fe/Si ratio was 0.05. After 2 h of microwave hydrothermal synthesis, few spherical crystallites appeared in the product as shown in Fig. 6(b), which should be attributed to the formation of Fe-containing hydrogarnet as evidenced in XRD results. Similar morphology was observed in literature as well [20]. However, after 4 h of microwave hydrothermal synthesis, few flakes were found to transfer to lamellar-shape crystallites as can be seen in Fig. 7(b), indicating the formation of Fe-tobermorite [23]. With the Fe/Si ratio at 0.1 (Figs. 6 and 7(c)), while few spherical crystals were still present, there was an increase in the lamellar-shape crystallites, suggesting the increasing of Fe-tobermorite. At an Fe/Si ratio of 0.15 (Figs. 6 and 7(d)), there was an apparent rise in spherical crystals number and a decrease in the presence of lamellar-shape crystals in the product, which was in line with the observation in XRD results. When the Fe/Si ratio is 0.2 (Figs. 6 and 7(e)), the

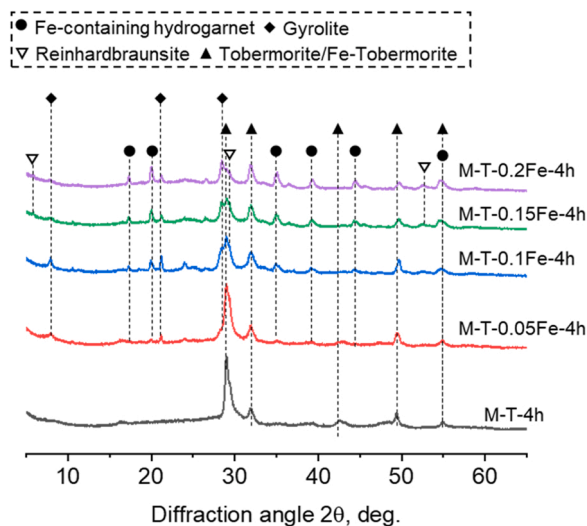


Fig. 4. XRD patterns of samples prepared with different ratios of Fe/Si after microwave hydrothermal synthesis for 4 h.

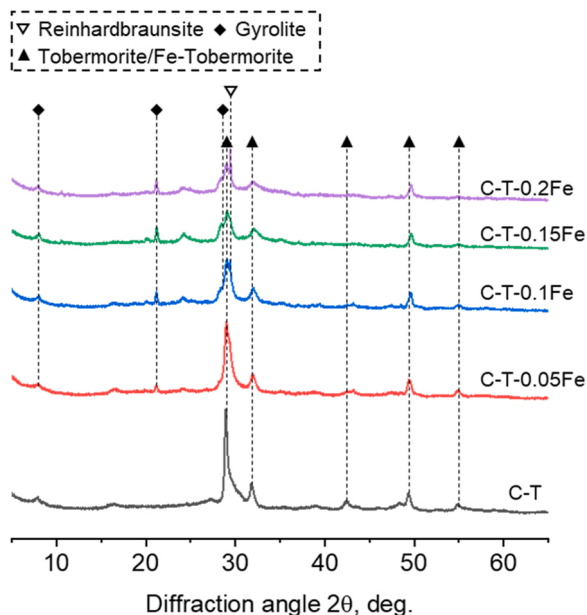


Fig. 5. XRD patterns of samples prepared with different ratios of Fe/Si after conventional hydrothermal synthesis for 14 h.

products showed agglomeration of crystallites.

SEM images of the samples made with different Fe/Si ratios at 14 h of conventional hydrothermal synthesis are shown in Fig. 8. As seen in Fig. 8(a), the sample morphology was fibrous which was another typical morphological habit of tobermorite [23]. At an Fe/Si ratio that was over 0.05, i.e. Fig. 8(b–e), the products were all in form of lamellar-shape crystallites, confirming the formation of Fe-tobermorite. It is worth noting that only limited amount of the spherical crystals could be observed in the products synthesized by conventional hydrothermal.

As evidenced by the formation of lamellar-shape crystals, it can thus be deduced that Fe successfully replaced the Si position in tobermorite to produce Fe-tobermorite during the hydration reaction. Additionally, under microwave hydrothermal synthesis, the products were mainly composed of Fe-tobermorite with a Fe/Si ratio of 0.1. With the rise of Fe/Si ratio, a dramatical increase in the formation of Fe-containing hydrogarnet was found. Whilst no significant difference was found in the morphologies of products under conventional hydrothermal synthesis among the different Fe/Si ratio (over 0.05).

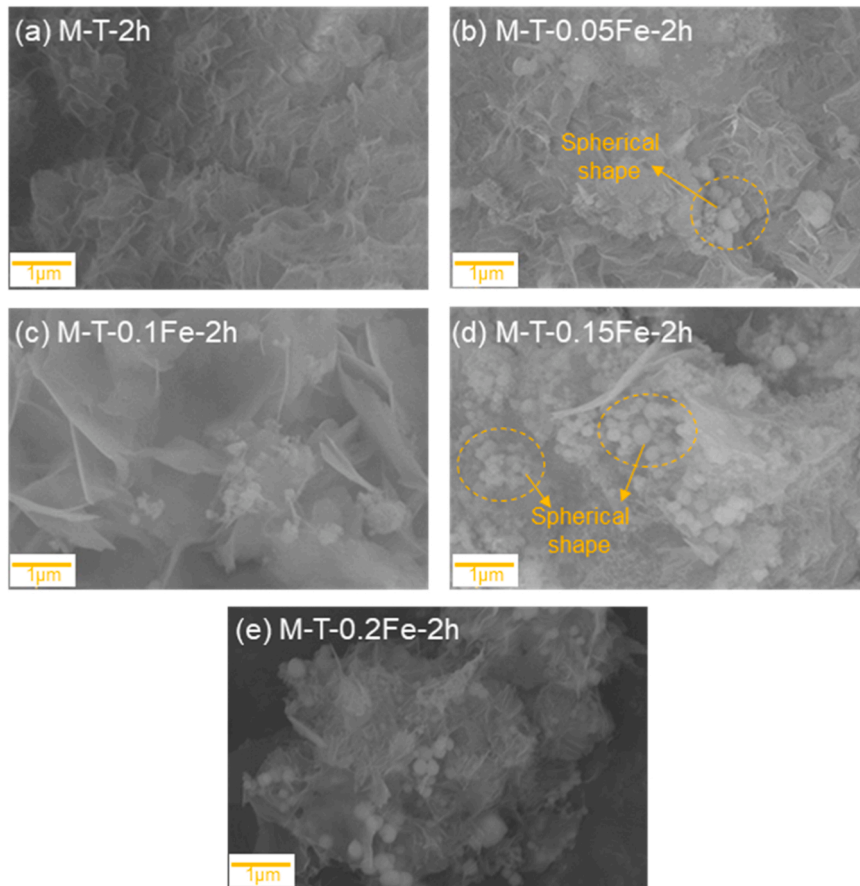


Fig. 6. SEM images of samples prepared with different ratios of Fe/Si after microwave hydrothermal synthesis for 2 h.

### 3.3. DTG: thermal properties of the products

The DTG plots of samples made with different Fe/Si ratios at 2 h and 4 h of microwave hydrothermal synthesis are shown in Figs. 9 and 10. The products synthesized after 2 h and 4 h microwave hydrothermal methods showed slightly different thermal behaviours. An exothermic peak at around 120 °C could be found in all samples, which was associated with the loss of interlayer water molecules in tobermorite/Fe-tobermorite [24,25]. The peak at around 245 °C was only observed in products that were synthesized with a Fe/Si ratio over 0.15, which should be attributed to the water loss of the Fe-containing hydrogarnet [26]. This result was in line with the XRD and SEM results, as there was an apparent increase in the amount of Fe-containing hydrogarnet when the Fe/Si ratio was over 0.15 [26]. Additionally, the DTG curves of all samples showed a peak at the range from 550 to 620 °C, corresponding to cleavage of the Si-O-H bonds in tobermorite/ Fe-tobermorite [26]. In Fig. 9, the position of the peak shifted from ~550 °C to ~600 °C when the Fe/Si ratio was increased from 0 to 0.05/0.1, which shifted back to ~550 °C with the further increase of the Fe/Si up to 0.2. It is thus suspected that the formation of the Fe-tobermorite had probably occupied the weak Si-O-H bond and left the remaining strong Si-O-H bonds. As can be seen that the amount of Fe-tobermorite reached the maximum at a Fe/Si ratio of 0.1, which decreased gradually with the increase of Fe/Si ratio. However, in Fig. 10, the peak was originally at around 620 °C which shifts to lower temperature gradually with the increase of Fe/Si ratio. The higher cleavage temperature for M-T-4 h sample should be benefited from its longer synthesis time, improving the degree of the crystallization of tobermorite [25]. With the addition of iron, the stability of Si-O-H bonds decreased since these bonds might have achieved the most stable status after 4 h of microwave hydrothermal synthesis. It is well known that tobermorite would transform to an anhydrous form of wollastonite ( $\text{CaSiO}_3$ ) at above 800 °C [26]. Therefore, an endothermic peak at ~800 °C was found in Fig. 9 for all samples. However, in Fig. 10, this peak shifted to a lower temperature at around 730 °C for the samples with addition of iron, which might be inferred as the larger amount of Fe-containing hydrogarnet formed.

The DTG curved confirmed the formation of Fe-tobermorite and Fe-containing hydrogarnet in the products with different Fe/Si ratio, and the maximum Fe-tobermorite can be obtained when the Fe/Si ratio was 0.05–0.1. Moreover, the products formed after 2 h of microwave hydrothermal synthesis were generally similar to those after 4 h, but the thermal behaviour exhibited slightly difference. Additionally, the stabilisation of Si-O-H bonds under high temperature would be reduced by the incorporation of Fe in tobermorite.

The DTG plots of samples made with different Fe/Si ratios at 14 h of conventional hydrothermal synthesis are shown in Fig. 11. 50–300 °C It is notable that there was only one exothermic peak at 100 °C, corresponding to the water loss of tobermorite for almost all

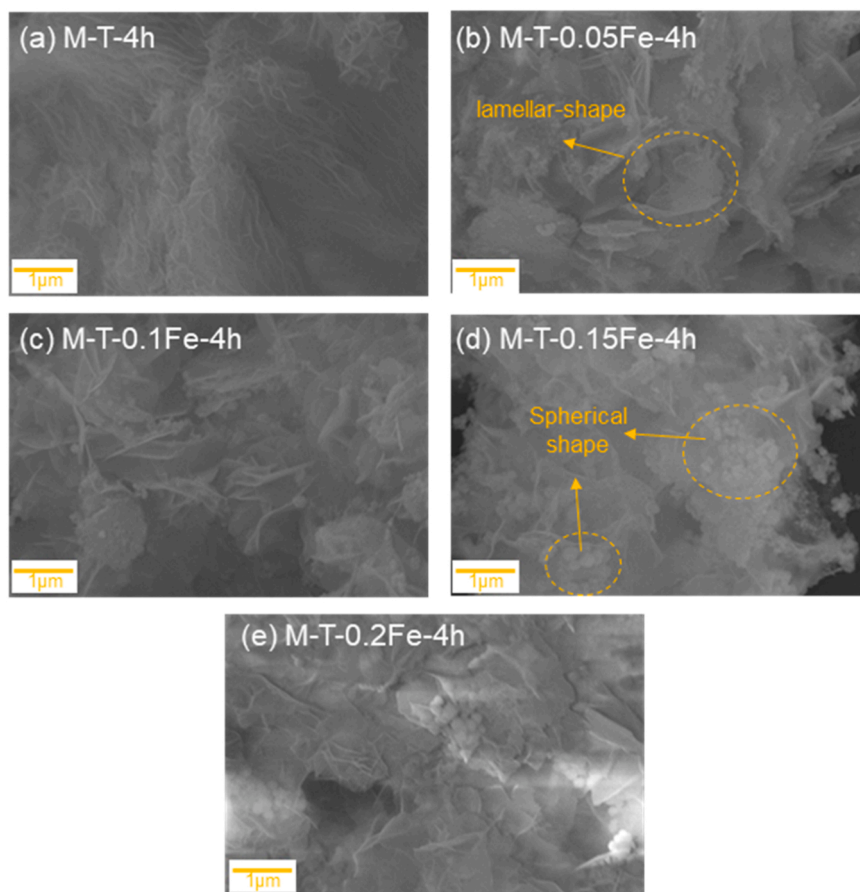


Fig. 7. SEM images of samples prepared with different ratios of Fe/Si after microwave hydrothermal synthesis for 4 h.

samples. Only the products synthesized with a Fe/Si ratio of 0.05 showed a broad peak at around 200 °C, which might have been caused by the formation of small amount of Fe-containing hydrogarnets as evidenced by SEM images in Fig. 8. The second exothermic peak related to the cleavage of Si-O-H bond at around (600 °C) was only observed in the products synthesized with a Fe/Si ratio less than 0.1, which should be attributed to the total transformation of tobermorite to Fe-tobermorite. A shift of peak to higher temperature could also be seen with the increase of the Fe/Si ratio, which was consistent with the previous observation under microwave hydrothermal synthesis. Overall, the cleavage of Si-O-H happened at a lower temperature than that produced by microwave hydrothermal synthesis, especially for the ones with high Fe/Si ratio. This should be linked to the formation of Fe-containing hydrogarnet as which was reported to be more stable than Fe-tobermorite [26]. With regard to the peak at around 800 °C indicating the formation of wollastonite, only a broad one could be seen in the products without any Fe in synthesis, and small peaks pointed by arrows in the figure for the products synthesized with Fe/Si ratio of 0.05/0.1.

#### 3.4. FTIR: Chemical bonds of the products

The FTIR results of the samples produced by different Fe/Si ratios at 2 h and 4 h of microwave hydrothermal synthesis and 14 h of conventional hydrothermal synthesis are shown in Figs. 12–14, respectively. Generally, the FTIR spectra of all products showed similar patterns with several peaks at the same positions, indicating the existence of certain chemical bonds regardless of the synthesis method and duration. For example, the peaks at 446  $\text{cm}^{-1}$  and 961  $\text{cm}^{-1}$  could be observed in all spectra, which were usually attributed to the stretching vibration modes of Si-O bonds [27,28]. But the intensities of these two peaks both reduced with the increase of the Fe/Si ratio, which should be induced by the increase of polymerization of silicate chains [28]. In addition to the peaks related to Si-O bonds, three peaks associated with C-O bonds could be found at 667, 876 and 1476  $\text{cm}^{-1}$  [27,29]. It is suspected to be caused by the carbonation of calcium compounds during the synthesis process while the samples were exposed to air as it has also been observed by other authors in the literature [28]. In higher range of wavenumber, the peaks at around 1638 and 3460  $\text{cm}^{-1}$  were present in all spectra which should be assigned to the vibrational mode of O-H bonds in  $\text{H}_2\text{O}$  molecular [9,27,28]. The only exception was the spectrum of the products synthesised with Fe/Si ration of 0.2 in conventional method which shifted to a lower wavenumber, indicating the strengthen of the O-H bond [30].



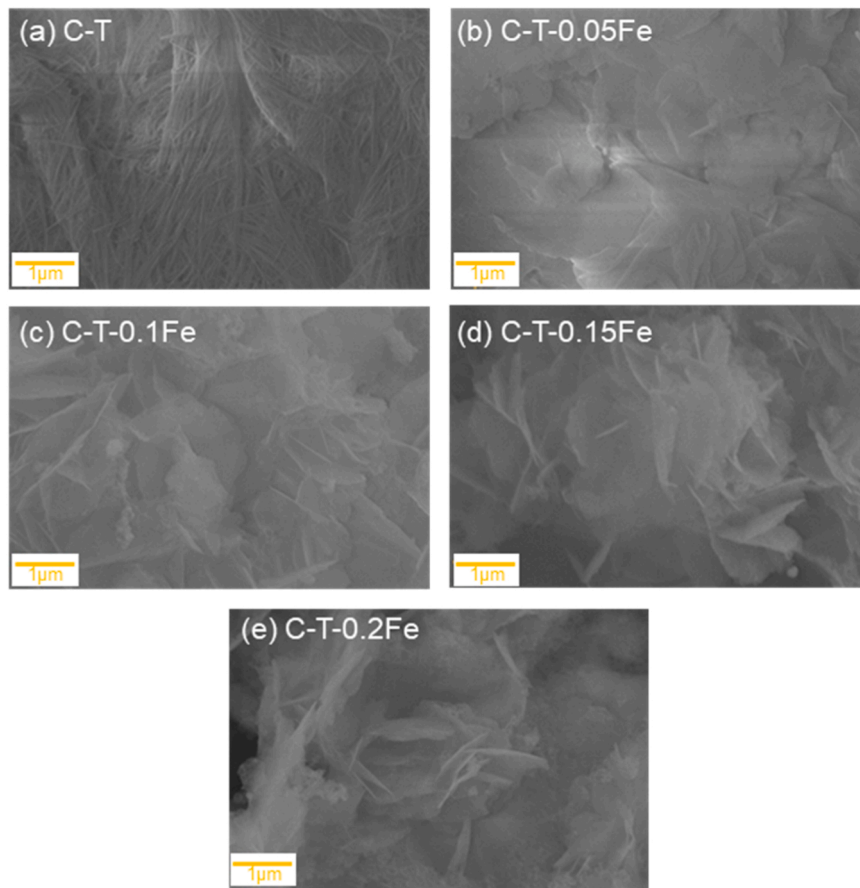


Fig. 8. SEM images of samples prepared with different ratios of Fe/Si after conventional hydrothermal synthesis for 14 h.

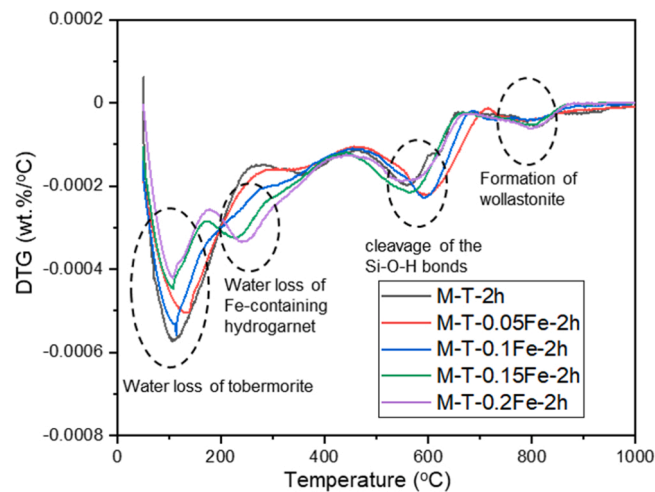


Fig. 9. TG-DTG diagram of samples prepared with different ratios of Fe/Si after microwave hydrothermal synthesis for 2 h.

Apart from the abovementioned peaks, there were some peaks only appeared when the products were synthesized with a Fe/Si ratio over 0. The peaks at around 588, 609 and 784  $\text{cm}^{-1}$  started to appear when the Fe/Si ratio was 0.05, whose intensities increased initially with the Fe/Si ratio increased to 0.1 and decreased afterwards until the Fe/Si ratio reached 0.2. These three peaks were related to the Si-O-Si bending, Si-O-Si symmetric stretching and Si-O-Si asymmetric stretching modes in silicate tetrahedra [9,29]. It could be found that the most intense peaks were both observed in the products when the Fe/Si ratio was 0.1. Additionally, the peaks at 997,

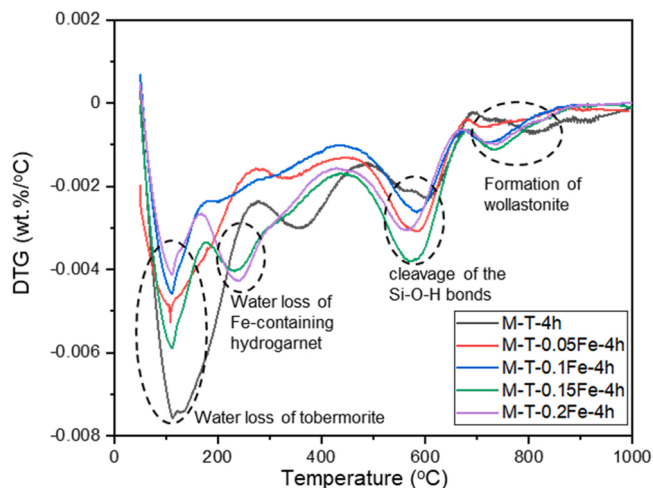


Fig. 10. TG-DTG diagram of samples prepared with different ratios of Fe/Si after microwave hydrothermal synthesis for 4 h.

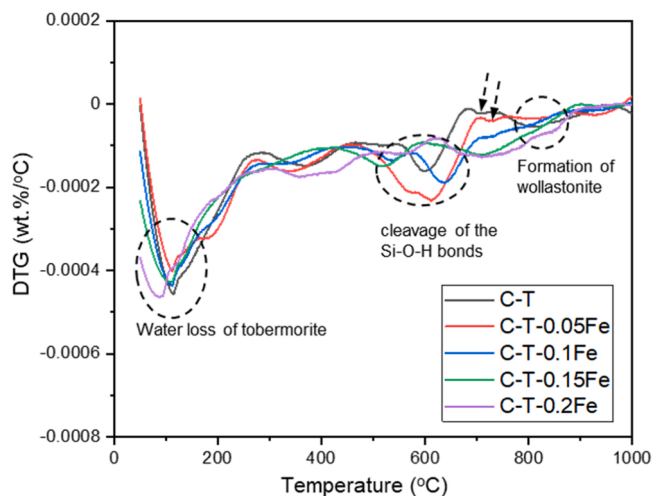


Fig. 11. TG-DTG diagram of samples prepared with different ratios of Fe/Si after conventional hydrothermal synthesis for 14 h.

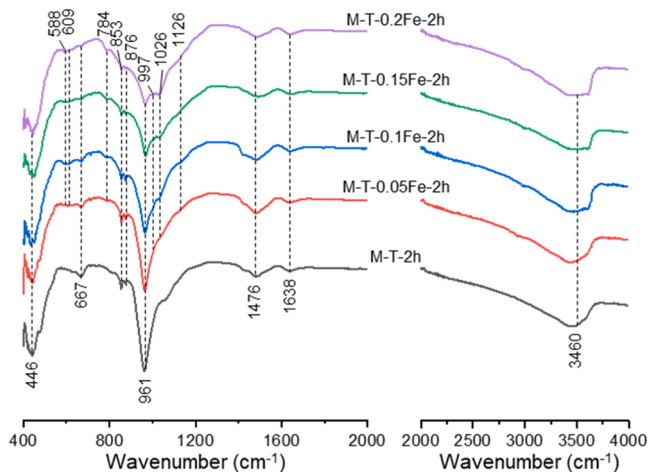


Fig. 12. FTIR diagram of samples prepared with different ratios of Fe/Si after microwave hydrothermal synthesis for 2 h.

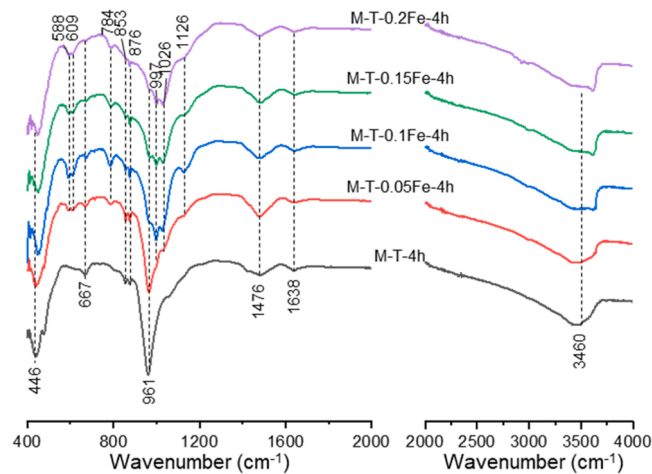


Fig. 13. FTIR diagram of samples prepared with different ratios of Fe/Si after microwave hydrothermal synthesis for 4 h.

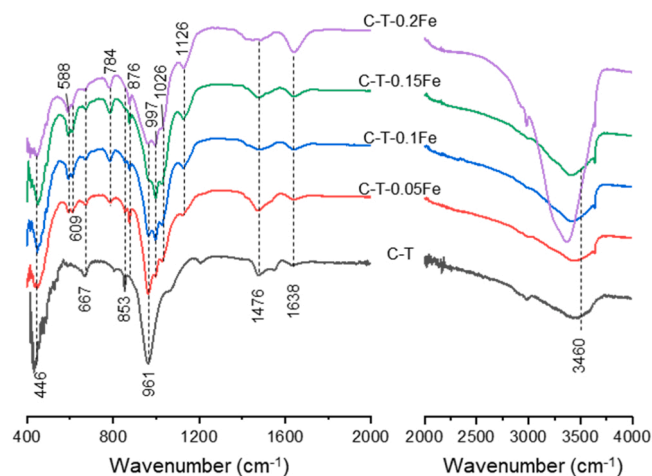


Fig. 14. FTIR diagram of samples prepared with different ratios of Fe/Si after conventional hydrothermal synthesis for 14 h.

1026 and 1126  $\text{cm}^{-1}$ , corresponding to vibrational modes of terminal Si-O bonds, showed a same trend, which appeared at a Fe/Si ratio of 0.05 and reached the maximum intensity at 0.1. As evidenced by SEM results, Fe-tobermorite reached the maximum amount at a Fe/Si ratio of 0.1. It is thus deduced that the Fe substitutions has increased the cross-linkage of silicate tetrahedra [9] and thus induced the increase in the intensities of these peaks. This could be used to explain the reduction of the intensities of these peaks when the Fe/Si ratio was further increased as the amount of the Fe-tobermorite decreased as can be seen in SEM results.

By comparing the FTIR spectra obtained from the samples produced by different methods and durations, the change of the peaks with different Fe/Si ratios were similar in all these three groups. In particular, the FTIR spectra in lower range from 400 to 2000  $\text{cm}^{-1}$  were almost identical for the one synthesized after 4 h of microwave hydrothermal and 14 h conventional hydrothermal. However, the spectra obtained from the samples from 2 h microwave hydrothermal synthesis showed the weakest peaks at 588, 609, 784, 997, 1026 and 1126  $\text{cm}^{-1}$ , especially for the products synthesized with the Fe/Si ratio at 0.01, implying the much better crystallization of Fe-tobermorite after 4 h of microwave hydrothermal synthesis.

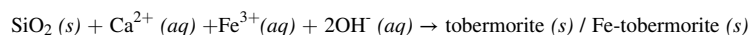
### 3.5. ICP-OES: solidification effectiveness of the products

The experimental results found that the iron concentrations in both supernatant and leaching solution were both comparable to that in a blank solution. Based on the absence of iron in the blank solution, it can be deduced that the concentration of iron was either undetectably low or completely absent, thereby suggesting that no iron existed in supernatant and leaching solution. On one hand, the absent of iron ions in supernatant implies that all iron has been successfully solidified in all products, even including the ones synthesized by microwave hydrothermal method for only 2 h. On the other hand, the missing of iron ions in leaching solution suggests the safety of the solidified body, i.e., products, which again includes the products produced after only 2 h of microwave hydrothermal

method. Therefore, 2 h are probably enough to solidify the iron by synthesizing tobermorite via microwave hydrothermal method, and the products were proved to be safe that would not leach any iron ions when the Fe/Si ratio was up to 0.2.

#### 4. Discussion

The overall reaction involved in the synthesis of tobermorite via both microwave/conventional hydrothermal methods is shown as follows [31],



The hydrothermal synthesis produces tobermorite, which is known as a layer structure with an inner calcium oxide layer and bridging tetrahedron outer layers [32]. While there are iron ions present, they would replace partial silicon ions at the outer layer to form Fe-tobermorite during the synthesis process [8–10].

The experimental results in present work showed that the variations in Fe/Si ratio could affect the synthesized products significantly, especially for the microwave hydrothermal synthesis. With the addition of Fe, Fe-tobermorite gradually formed as evidenced in the SEM results in present work, which was in line with the observation in the literature [20]. In addition to Fe-tobermorite, gyrolite also appeared with the increase of Fe/Si ratio, which should be attributed to the increase of Ca/Si ratio in the raw material since the phase of products to be formed is theoretically dependent on the Ca/Si ratio [33]. More notably, Fe-containing hydrogarnet in spherical shape was only observed in the products via microwave hydrothermal synthesis. This might be owed to the combined effects of the increase in the Fe containment and enhancement of the mass transfer under microwave [33]. The presence of gyrolite during the solidification process is generally deemed to have negligible or slightly adverse consequences, as evidenced by the lack of solidified iron, whilst the formation of Fe-containing hydrogarnet exhibits a positive effect due to the successful solidification of iron. The presence of tobermorite holds inherent value due to its capacity to effectively solidify a substantial majority of iron ions. Additionally, the products via microwave hydrothermal method showed a better resistance to high temperature with a more stable Si-O-H bond.

Despite the difference in the chemical compositions of the final products, the microwave hydrothermal synthesis exhibited a much more effective performance by comparing with conventional method in terms of the solidification of Fe. Only 2 h were required for microwave hydrothermal synthesis to solidify all Fe even when the Fe/Si ratio was up to 0.2. Such an improvement in the efficiency of solidification should be attributed to the rapid heating up of the entire reaction system evenly [34], which is benefited from the nature of microwave. Microwave heating transfers the energy directly to the molecular bonds within material through electric field with extremely deep penetration [34]. The energy would then induce the vibration of molecular bonds and thus heat up the entire system thoroughly much faster than conventional heating method. In addition to thermal effect, microwave heating is famous for its non-thermal effect [34]. Specifically, the microwave field provides a non-linear driving force for the ions in the system [34], effectively enhancing the mass transfer rate and thus reducing the activation energy for the hydrothermal process.

Considering the economic benefits by using microwave hydrothermal synthesis, the energy consumption of both methods, microwave and conventional ones, for synthesising tobermorite to solidify iron is shown Table 3. It can be seen that there is a dramatical drop in the energy consumption by replacing the conventional method with the microwave heating. In particular, compared with conventional hydrothermal synthesis for 14 h, a significant reduction (95.2 %) in energy consumption has been achieved from microwave hydrothermal synthesis for 2 h, demonstrating a remarkable potential to benefit the cost for solidification as well as its environmental impact.

To further develop the microwave hydrothermal synthesis of tobermorite for the solidification of iron, it is suggested that the time for the microwave hydrothermal synthesis can be further reduced as 100 % Fe solidification might have achieved before 2 h. In the meantime, the Fe/Si ratio can be increased to further evaluate the capacity of Fe that can be solidified via microwave hydrothermal synthesis of tobermorite. Regarding the potential of this technique for industrial-scale development, one key aspect of scaling up microwave utilization is the availability of appropriate equipment and infrastructure. Fortunately, industrial-scale microwave reactors capable of handling larger volumes and higher temperatures are already available in the market. However, there are still several challenges to be addressed before practical scale-up, such as process optimization, safety and economic feasibility. While scaling up microwave utilization for industrial applications may present certain challenges, many of these can be addressed through careful planning, optimization, and advancements in technology.

#### 5. Conclusion

This work demonstrated the feasibility of microwave hydrothermal synthesis for the solidification of Fe. Different chemical and physical properties of the products synthesized under microwave and conventional hydrothermal synthesis were characterized and compared, and the efficiency of these two methods to solidify Fe was evaluated. The main conclusion can be drawn:

**Table 3**  
Energy consumption under different heating methods.

Method	Power of Instrument (kW)	Heating Time to 220 °C (h)	Holding time (h)	Total Energy Consumption (kW h)
Conventional heating	1.5	0.66	14	21.99
Microwave heating	0.45	0.36	4	1.96
			2	1.06

- The dominant product produced under conventional hydrothermal synthesis were Fe-tobermorite/tobermorite, along with gyrolite and reinhardbraunsite. In addition to these compounds, Fe-containing hydrogarnet was also formed under microwave hydrothermal synthesis. In particular, the dominant compounds switched from Fe-tobermorite/tobermorite to Fe-containing hydrogarnet with the increase of Fe/Si ratio.
- The products formed under microwave hydrothermal synthesis demonstrated a more stable state under high temperature than that produced via conventional hydrothermal synthesis, which was benefited from the dominant compounds, Fe-containing hydrogarnet.
- Both microwave and conventional hydrothermal synthesis of tobermorite can effectively solidify iron ions by chemical substitution by 100 % when the Fe/Si ratio was up to 0.2. More importantly, the microwave hydrothermal synthesis was more effective as it only required one-seventh of time to achieve the sample solidification efficiency as conventional hydrothermal synthesis in present work.

Consequently, our results suggest that microwave hydrothermal synthesis of tobermorite is a promising technique to solidify iron ions with superior efficiency and more stable products by compared with conventional hydrothermal synthesis.

### Declaration of Competing Interest

The authors declare that they have no known competing financial interests or personal relationships that could have appeared to influence the work reported in this paper.

### Data Availability

Data will be made available on request.

### Acknowledgements

The authors all thank the financial supports from the National Foreign Experts Project (G2021026031L), the National Natural Science Foundation of China (52278256, 51808196), the Doctor Fund from Henan Polytechnic University (B2021-15), the Post-doctoral Fund from Henan Polytechnic University (672108/106), the Fund for the Innovative Research Team of Henan Polytechnic University in 2023 (T2023-5), the Fundamental Research Funds for the Universities of Henan Province (SFRF220418) and Henan Outstanding Foreign Scientists' Workroom (GZS2021003).

### References

- [1] Z. Fu, F. Wu, L. Chen, B. Xu, C. Feng, Y. Bai, H. Liao, S. Sun, J.P. Giesy, W. Guo, Copper and zinc, but not other priority toxic metals, pose risks to native aquatic species in a large urban lake in Eastern China, *Environ. Pollut.* 219 (2016) 1069–1076.
- [2] B. Rusch, K. Hanna, B. Humbert, Coating of quartz silica with iron oxides: Characterization and surface reactivity of iron coating phases, *Colloids Surf. A-Physicochem. Eng. Asp.* 353 (2–3) (2010) 172–180.
- [3] R.R. Navarro, S. Wada, K. Tatsumi, Heavy metal precipitation by polycation-polyanion complex of PEI and its phosphonomethylated derivative, *J. Hazard. Mater.* 123 (1–3) (2005) 203–209.
- [4] None, Preparation of monolith-type catalyst for methanol steam reforming: M. Shimomura; S. Nojima Mitsubishi Heavy Industries Ltd Jpn Kokai Tokkyo Koho 87,61,643; Mar. 18, 1987; Appl. Sept. 11, 1985, 8(4) , 1988, pp. 341–0.
- [5] I.G. Richardson, The calcium silicate hydrates, *Cem. Concr. Res.* 38 (2) (2008) 137–158.
- [6] G. Geng, R.J. Myers, J. Li, R. Maboudian, C. Carraro, D.A. Shapiro, P.J.M. Monteiro, Aluminum-induced dreierketten chain cross-links increase the mechanical properties of nanocrystalline calcium aluminosilicate hydrate, *Sci. Rep.* 7 (1) (2017) 44032.
- [7] S. Merlino, E. Bonaccorsi, T.J. Armbruster, Tobermorites: Their real structure and order-disorder (OD) character, *Am. Mineral.* 84 (10) (1999) 1613–1621.
- [8] E.I. Al-Wakeel, S.A. El-Korashy, S.A. El-Hemaly, M.A. Rizk, Divalent ion uptake of heavy metal cations by (aluminum + alkali metals) – substituted synthetic 1.1 nm-tobermorites, *J. Mater. Sci.* 36 (10) (2001).
- [9] N.Y. Mostafa, E.A. Kishar, S.A. Abo-El-Enein, FTIR study and cation exchange capacity of Fe<sup>3+</sup>- and Mg<sup>2+</sup>-substituted calcium silicate hydrates, *J. Alloy. Compd.* 473 (1–2) (2009) 538–542.
- [10] Xiaoqin Peng, Luping Tang, Lu Zeng , Shuping Wang , Cong, Influence of inorganic admixtures on the 11 A-tobermorite formation prepared from steel slags: XRD and FTIR analysis, *Constr. B. Mater.*, 2014.
- [11] T. Tsutsumi, S. Nishimoto, Y. Kameshima, M. Miyake, Hydrothermal preparation of tobermorite from blast furnace slag for Cs<sup>+</sup> and Sr<sup>2+</sup> sorption, *J. Hazard. Mater.* 266 (2014) 174–181.
- [12] J. Ding, Z. Tang, S. Ma, Y. Wang, S. Zheng, Y. Zhang, S. Shen, Z. Xie, A novel process for synthesis of tobermorite fiber from high-alumina fly ash, *Cem. Concr. Compos.* 65 (2016) 11–18.
- [13] X. Huang, D. Jiang, S. Tan, Novel hydrothermal synthesis method for tobermorite fibers and investigation on their thermal stability, *Mater. Res. Bull.* 37 (11) (2002) 1885–1892.
- [14] T. Yeur-Luen, C.M. L, P.N. J, M.S. J, Synthesis and electrical characterization of thin films of PT and PZT made from a diol-based sol-gel route, *J. Am. Ceram. Soc.* 79 (2) (1996) 441–448.
- [15] V.B. Yu, K.I. Rybakov, V. Semenov, High-temperature microwave processing of materials, *J. Phys.* 34 (13) (2001) R55–R75.
- [16] T. Gerdes, M. Whxert-Porada, Microwave Sintering of Metal-Ceramic and Ceramic-Ceramic Composites, *MRS Online Proc. Lib.* 347 (1994) 531.
- [17] S. Komarneni, J.S. Komarneni, B. Newalkar, S. Stout, Microwave-hydrothermal synthesis of Al-substituted tobermorite from zeolites, *Mater. Res. Bull.* 37 (6) (2002) 1025–1032.
- [18] M. Miyake, S. Niiya, M. Matsuda, Microwave-assisted Al-substituted tobermorite synthesis, *J. Mater. Res.* 15 (4) (2000) 850–853.
- [19] J. Chang, Study on microwave hydrothermal synthesis of tobermorite Civil Engineering, Henan Polytechnic University, Henan, China, 2021.
- [20] J. Siramanont, B.J. Walder, L. Emsley, P. Bowen, Iron incorporation in synthetic precipitated calcium silicate hydrates, *Cem. Concr. Res.* 142 (2021), 106365.
- [21] W. Chen, J. Qian, J. Liu, C. Xie, Y. Lei, H. Luo, Solidification and leaching stability of heavy metals in sintered products made of shale and sewage sludge, *J. Chin. Ceram.* 40 (10) (2012) 1420–1426.

- [22] C. Zeng, Y. Lyu, D. Wang, Y. Ju, X. Shang, L. Li, Application of Fly Ash and Slag Generated by Incineration of Municipal Solid Waste in Concrete, *Adv. Mater. Sci. Eng.* 2020 (2020) 7802103.
- [23] N.Y. Mostafa, A.A. Shaltout, H. Omar, S.A. Abo-El-Enein, Hydrothermal synthesis and characterization of aluminium and sulfate substituted 1.1nm tobermorites, *J. Alloy. Compd.* 467 (1) (2009) 332–337.
- [24] A. Majdinasab, Q. Yuan, Synthesis of Al-substituted 11Å tobermorite using waste glass cullet: A study on the microstructure, *Mater. Chem. Phys.* 250 (2020), 123069.
- [25] L. Galvánková, J. Másilko, T. Solný, E. Štěpánková, Tobermorite synthesis under hydrothermal conditions, *Procedia Eng.* 151 (2016) 100–107.
- [26] B.Z. Dilnesa, B. Lothenbach, G. Renaudin, A. Wichser, D. Kulik, Synthesis and characterization of hydrogarnet  $\text{Ca}_3(\text{Al}_x\text{Fe}_{1-x})_2(\text{SiO}_4)_y(\text{OH})_4(3-y)$ , *Cem. Concr. Res.*, 59, 2014, pp. 96–111.
- [27] I.G. Lodeiro, D.E. Macphee, A. Palomo, A.J.C. Fernández-Jiménez, C. Research, Effect of alkalis on fresh C–S–H gels, *FTIR Anal.* 39 (3) (2009) 147–153.
- [28] P. Yu, R.J. Kirkpatrick, B. Poe, P.F. McMillan, X. Cong, Structure of calcium silicate hydrate (C-S-H): Near-, Mid-, and Far-infrared spectroscopy, *Am. Ceram. Soc.*, 82(3), 1999, pp. 742–748.
- [29] I. García-Lodeiro, A. Fernández-Jiménez, M.T. Blanco, A. Palomo, FTIR study of the sol–gel synthesis of cementitious gels: C–S–H and N–A–S–H, *J. Sol-Gel Sci. Technol.* 45 (1) (2008) 63–72.
- [30] F. Cheng, Q. Cao, Y. Guan, H. Cheng, X. Wang, J.D. Miller, FTIR analysis of water structure and its influence on the flotation of arcanite ( $\text{K}_2\text{SO}_4$ ) and epsomite ( $\text{MgSO}_4 \cdot 7\text{H}_2\text{O}$ ), *Int. J. Miner. Process.* 122 (2013) 36–42.
- [31] S.A. Greenberg, Reaction between silica and calcium hydroxide solutions. I. Kinetics in the temperature range 30 to 85°, *J. Phys. Chem.* 65 (1) (1961) 12–16.
- [32] N. Zhang, P. Carrez, R.J.Aam Shahsavari, interfaces, Screw-dislocation-induced strengthening–toughening mechanisms in complex layered materials: The case study of tobermorite, 9(2), 2017, pp. 1496–1506.
- [33] R. Šiauciunas, K. Baltakys, Formation of gyrolite during hydrothermal synthesis in the mixtures of CaO and amorphous  $\text{SiO}_2$  or quartz, *Cem. Concr. Res.* 34 (11) (2004) 2029–2036.
- [34] A.G. Whittaker, Diffusion in microwave-heated ceramics, *Chem. Mater.* 17 (13) (2005) 3426–3432.